Multizone Rapid Thermal Processing to Overcome Challenges in Carbon Nanotube Manufacturing by Chemical Vapor Deposition

Jaegeun Lee
Department of Industrial Engineering, University of Pittsburgh, Pittsburgh, PA, USA
Moataz Abdulhafez
Department of Industrial Engineering, University of Pittsburgh, Pittsburgh, PA, USA
Mostafa Bedewy*
Department of Industrial Engineering, Department of Chemical and Petroleum Engineering
Department of Mechanical Engineering and Materials Science, University of Pittsburgh
Pittsburgh, PA, USA
*Corresponding author.
E-mail address: mbedewy@pitt.edu

Abstract

For the scalable production of commercial products based on vertically aligned carbon nanotubes (VACNTs), referred to as CNT forests, key manufacturing challenges must be overcome. In this work, we describe some of the main challenges currently facing CNT forest manufacturing, along with how we address these challenges with our custom-built rapid thermal processing chemical vapor deposition (CVD) reactor. First, the complexity of multistep processes and reaction pathways involved in CNT growth by CVD limits the control on CNT population growth dynamics. Importantly, gas-phase decomposition of hydrocarbons, formation of catalyst nanoparticles, and catalytic growth of CNTs are typically coupled. Here, we demonstrated a decoupled recipe with independent control of each step. Second, significant run-to-run variations plague CNT growth by CVD. To improve growth consistency, we designed various measures to remove oxygen-containing molecules from the reactor, including air baking between runs, dynamic pumping down cycles, and low-pressure baking before growth. Third, real-time measurements during growth are needed for process monitoring. We implement *in situ* height kinetics via videography. The combination of approaches presented here has the potential to transform lab-scale CNT synthesis to robust manufacturing processes.

1. Introduction

Carbon nanotubes (CNTs) are allotropes of carbon with cylindrical structures and nanoscale diameters. They are unique nanomaterials, because individual CNTs possess exceptionally high electrical [1] and thermal [2] conductivity as well as high mechanical strength [3]. When CNTs are grown on a substrate at high areal number density, they self-organize and form a vertically aligned structure, which is often called a "CNT forest".

2

Journal of Manufacturing Science and Engineering. Received May 07, 2019; Accepted manuscript posted May 13, 2019. doi:10.1115/1.4044104

Copyright © 2019 by ASME

The high density and alignment of CNT forests combined with the properties of individual

CNTs make them promising for applications that leverage their collective properties, such as

thermal interfaces [4], electrical interconnects [5], flow membranes [6], and structural materials

[7].

Over the past two decades, significant progress in CNT forest growth has been achieved. In

terms of height, for example, the first CNT forest grown in 1999 had a height of 0.24 mm [8],

and now the growth of up to 21.7 mm tall CNT forests is possible [9]. Figure 1 summarizes

some of the representative CNT forest growth results over the years. This progress was

accompanied by better understanding of various aspects of the growth process, including the

effects of growth promoters like water vapor [10], the pathways for catalyst migration during

growth [11], and the mechanisms of catalytic deactivation and growth termination [12].

Despite the abovementioned advances however, the commercialization of products based on

CNT forests has been largely limited. Several major issues still plague the development of

scalable and robust CNT forest manufacturing processes.

In this paper, we describe the main challenges currently limiting the manufacturing of CNT

forests, and we propose our approaches towards addressing these challenges, leveraging a

unique custom-built rapid thermal processing chemical vapor deposition (RTP-CVD) reactor.

Finally, we will demonstrate through experimental results our ability to overcome the

challenges of CNT forest manufacturing by CVD.

2. Challenges in CNT forest manufacturing

One of the obvious challenges in manufacturing CNT forests is the scalability issue in lab-scale

3

CVD reactors. Nevertheless, recent progress in roll-to-roll and continuous processing [13,14]

as well as in floating catalyst growth [15] indicates that high-throughput and continuous

processes are possible and can be implemented in industrial scale production. On the other

hand, there are still some major roadblocks that will only be overcome with a better

understanding of the complex physicochemical processes involved in CNT forest growth.

A CNT forest is population of CNTs, typically exceeding tens of billions of CNTs per square

centimeter, which grow simultaneously. Hence, controlled growth of CNT forests in terms of

density, alignment, size distribution, and height is of great importance for their successful

commercialization. In this paper, we focus on the following three specific challenges that still

require fundamental research into CNT forest growth.

2.1. Complexity and coupling of physicochemical processes

CVD growth of CNT forests proceeds in multiple successive steps that are often coupled. A

thin film catalyst is typically first prepared by the deposition of transition metals such as iron

or nickel on a solid substrate. Prior to growth, the catalyst-coated substrate is thermally treated

in a reducing atmosphere to form catalytically active nanoparticles on the substrate. For the

growth of CNTs, a hydrocarbon gas is supplied as carbon source. The hydrocarbon goes

through gas-phase decomposition at high temperature, and the decomposed gas-phase species

travels to the catalyst-coated substrate. Finally, carbon atoms from the active species self-

organize on catalyst nanoparticles and get incorporated into the growing CNTs.

What makes the situation more complex is the fact that these component steps are coupled in

typical reactor systems. In most reactors, there is only a single reaction zone where the thermal

and chemical treatment of the catalyst, the gas-phase decomposition of hydrocarbon gas, and

the catalytic growth of CNTs occur. Thus, conditions such as pressure, temperature and gas

4

MANU-19-1275, Bedewy

Downloaded From: https://manufacturingscience.asmedigitalcollection.asme.org on 06/27/2019 Terms of Use: http://www.asme.org/about-asme/terms-of-use

chemistry for these reactions are coupled.

Recognizing the importance of independent control of gas-phase reaction, previous efforts have been exerted towards decoupling the gas-phase reaction from CNT growth [16–21]. In those reports, usually a separate preheater was used, which resulted in the growth at lower substrate temperatures. For example, with the help of a preheating zone, Thompson et al. reported the growth of CNT forests at a temperature as low as 475 °C [19]. Park et al. employed a temperature gradient CVD where the temperature profile of the gas phase was controlled by the temperature of the top and bottom heaters [20,21]. Meshot et al. suggested that certain carbon species generated from gas-phase reaction either enhance or inhibit CNT growth [18]. In addition, the formation of catalyst particles is coupled with catalytic growth of CNTs. Usually, the growth step immediately follows the catalyst formation step. In fact, the catalyst formation step determines the CNT forest density because the properties of the population of catalyst nanoparticles (i.e. size distribution of the catalyst nanoparticles and areal number density) are determined in this step. Nevertheless, in most cases, the conditions for catalyst formation are bound to that of CNT growth as the two steps are sequentially adjacent processes. There have been only few research efforts aimed at decoupling the catalyst formation step from CNT growth. Hata et al. decoupled the catalyst formation by using rapid thermal processing [22,23]. Hart et al. worked on decoupling the catalyst formation step by using a magnetically

In sum, the complexity and coupled nature of growth in the conventional reactors limits independent optimization of process parameters for individual steps of the process.

actuated transfer arm to move the substrate rapidly into and out of the CVD reactor [24].

2.2. Run-to-run variation

For commercial production, high consistency in manufacturing must be achieved through

Journal of Manufacturing Science and Engineering. Received May 07, 2019; Accepted manuscript posted May 13, 2019. doi:10.1115/1.4044104

Copyright © 2019 by ASME

statistical process control. Without securing this statistical consistency, any efforts to perform

parametric optimization can be overwhelmed by other uncontrollable variations. Unfortunately,

however, it is widely observed that the growth of CNTs lacks consistency [25].

Inconsistency originates from the high degree of sensitivity to oxygen-containing molecule in

the reactor. Noy et al. reported that trace amount of water vapor (~ 1 ppm) can significantly

affect the growth [26,27]. Plata et al. showed different growth behaviors with different

concentrations of oxygen. They pointed out that a low concentration of oxygen can accelerate

the Ostwald ripening of Fe nanoparticles [28]. Therefore, it is imperative that we actively

secure consistent growth, although oxygen-containing molecules easily adsorb to reactor walls.

2.3. Dynamic CNT population behavior

Researchers studying growth mechanisms usually simplify the growth by assuming a perfectly

uniform group of identical nanotubes, and explain the behavior based on a single CNT-catalyst

system. However, this limits the precise understanding of the spatiotemporal evolution of CNT

forests during growth, which is another major obstacle. CNTs growing together in a forest are

not monodisperse in diameter, but rather exhibit significant polydispersity of sizes and growth

rates while being mechanically coupled [29–34].

So far, various ex situ and in situ characterizations methods have been utilized to build our

understanding of the collective growth behavior of CNT forests. For example, ex situ

characterization by synchrotron X-ray scattering explained the frequently observed abrupt

growth termination behavior via a collective growth model [33] and revealed the diameter-

dependent kinetics [34]. In situ transmission electron microscopy study demonstrated the

mechanical coupling between CNTs [31]. To gain better control over the process-structure-

property relationship governing CNT forest applications, the stochastic nature of the CNT

MANU-19-1275, Bedewy

Downloaded From: https://manufacturingscience.asmedigitalcollection.asme.org on 06/27/2019 Terms of Use: http://www.asme.org/about-asme/terms-of-use

growth as a population must be comprehensively understood.

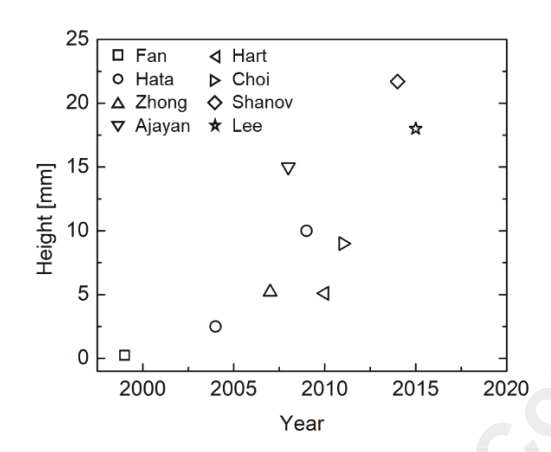


Figure 1. Height of representative CNT forests. References: Fan 1999 [8], Hata 2004 [10], Zhong 2007 [35], Ajayan 2008 [36], Hata 2009 [37], Hart 2010 [38], Choi 2011 [39], Shanov 2014 [9], and Lee 2015 [40].

3. Approaches to address the challenges

3.1. Decoupled recipe

To address growth complexity, we decouple the multiple coupled steps of the CNT growth. We design dynamic growth recipes, in which gas-phase decomposition of hydrocarbon precursor, catalyst formation, and catalytic growth of CNTs are independently controlled.

3.2. Robust process

To enhance the robustness of the growth process and reduce its sensitivity to uncontrolled concentrations of chemical species, we ensure the condition of the reactor is identical before every growth run. Towards that goal we employed the following: (1) air baking between runs,

7

(2) pumping down before the recipe, and (3) low-pressure baking before growth.

3.3. In situ measurements

To investigate the population dynamics of CNTs, a precise measurement of the growth kinetics

is required. In our system, CNT forest growth is recorded by a camera connected to a computer.

Through image processing, in situ height kinetics for each experiment is measured.

4. Unique capabilities of our reactor

The approaches described above for overcoming challenge in CNT forest growth can be

realized only when we are equipped with a reactor that provides unique process control. Our

custom-designed RTP-CVD reactor shown in Figure 2 enables us to achieve this goal based on

the following features:

• Reactor consists of two adjacent furnaces: a resistive preheater for thermal

decomposition of hydrocarbon precursors (supplied through a coiled injector) and an

infrared (IR) heater for catalyst treatment and CNT growth.

• IR heater has 3-zone control along the axis as well as independent control of top and

bottom lamps, to create thermal gradients and achieve fast heating (> 50 °C/s).

• A viewing port enables in situ height kinetics measurements

Programmed dynamic recipes are automated.

• The growth data (e.g. time evolution of temperature, pressure, gas flow rates, etc.) are

recorded for analytics

• The addition of H₂O is well controlled via a bubbler with accurate temperature and

8

pressure control.

- A variety of gases (He, H₂, C₂H₂, C₂H₄, CH₄) are used.
- Vacuum pump for purging and air pump for bake-cleaning.

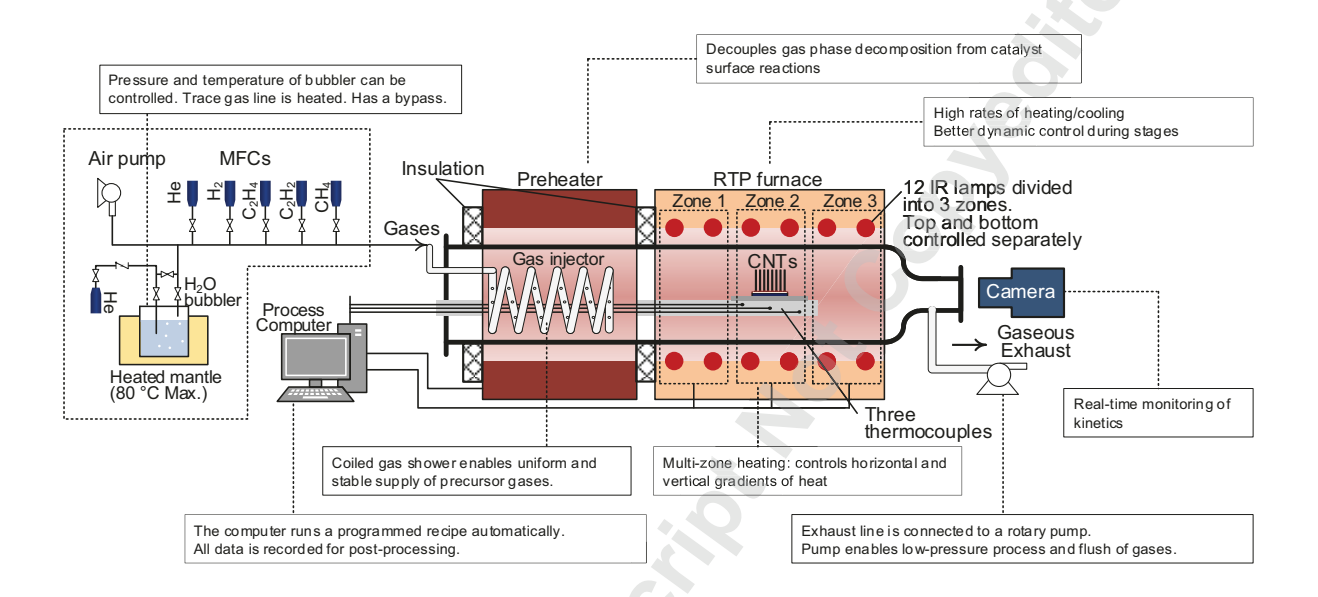


Figure 2. Schematic representation of our custom-designed rapid thermal processing CVD reactor.

5. Experimental

A SiO_2 (300 nm) coated Si wafer was used as a substrate. The substrate was coated with 10 nm of AlO_x layer by atomic layer deposition and then, 1 nm of Fe layer was deposited by e-beam evaporation. The substrate was cut into 5-10 mm pieces for each growth of CNT forest.

When the substrate is loaded into our custom-designed reactor (CVD Equipment, Central Islip, NY), a preprogrammed recipe automatically starts to run. The detailed information of each

Journal of Manufacturing Science and Engineering. Received May 07, 2019; Accepted manuscript posted May 13, 2019. doi:10.1115/1.4044104

Copyright © 2019 by ASME

recipe is given in the appropriate figure below.

Height of each CNT forest was measured by optical microscope. Since there was some spatial

variation of the height, we measured height from 6 points on two sides of each sample and

averaged the values.

6. Decoupling of gas-phase reaction

First, we decoupled the gas-phase reaction from CNT growth. This was enabled by use of the

separate preheater. The gas molecules are heated as they travel inside the resistive preheater

and go through complex chemical reactions in the gas phase. In contrast, the gas molecules

traveling the growth zone is not heated by IR in the growth zone. Thus, the gas-phase reaction

is solely controlled in the preheater, which means a nearly complete decoupling of gas-phase

reaction.

Rigorously speaking, our method to decouple gas-phase reaction is the closest to ideal

decoupling of gas-phase reaction. In some previous reports [16–21], even though a separate

preheater was used, the main reactor was usually hot-walled, so it was impossible to avoid

additional gas-phase reactions in the CNT growth zone. Using a cold-walled IR heater in the

main growth zone, minimizes the gas-phase reaction this zone. In addition, if the preheater is

further upstream from the main reactor, the pre-decomposed hydrocarbon is cooled down and

goes through recombination [18]. In our system, the preheater is directly adjacent to the main

reactor to prevent this phenomenon.

The effect of gas-phase reaction is shown in Figure 3. Having other conditions equal, only the

temperature of preheater during the growth step was varied. The detailed information of the

10

MANU-19-1275, Bedewy

 $Downloaded\ From:\ https://manufacturingscience.asmedigital collection.asme.org\ on\ 06/27/2019\ Terms\ of\ Use:\ http://www.asme.org/about-asme/terms-of-use$

representative recipes is displayed in Figure 3a and b. The effect of preheater temperature is clearly shown in Figure 3c. The growth was dramatically improved when the temperature of preheater went above 800 °C. The high sensitivity of the growth to the preheater temperature indicates that the decoupling of gas-phase reaction was successful. The results also support the previous finding that gas-phase reaction critically affects the overall growth kinetics [18,21,41]. This high sensitivity is consistent with the results by Nessim et al [19]. Considering that the height of the CNT forests reported was less than 1 μ m, our result is a generalization of the phenomenon at a much larger length scale (hundreds of micrometers).

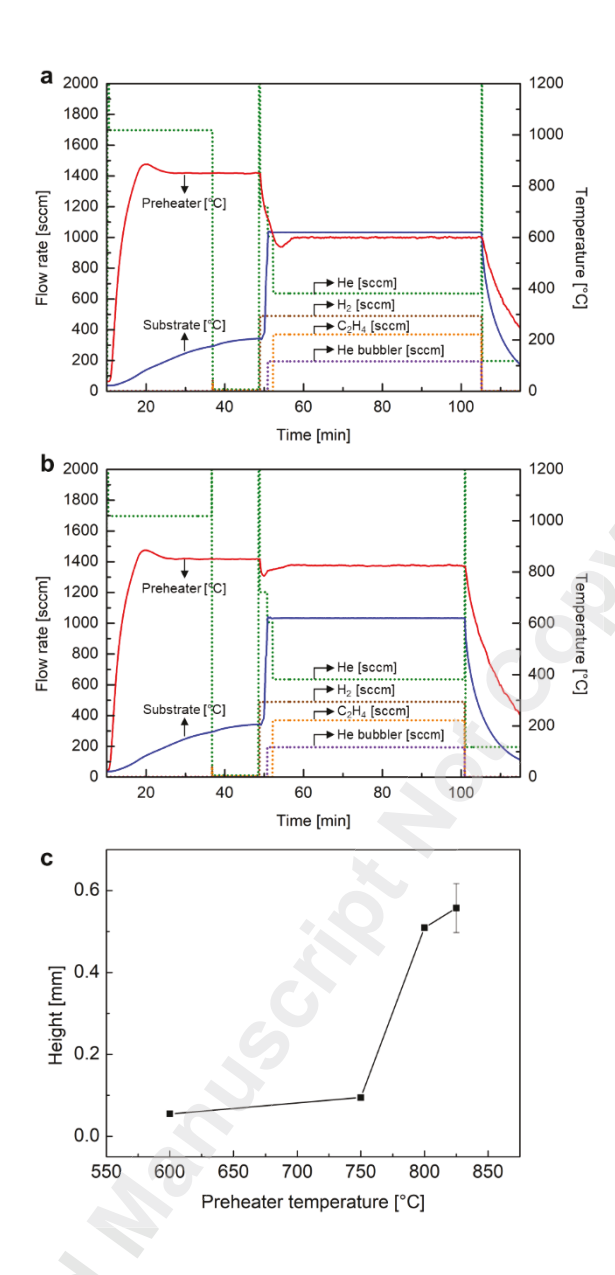


Figure 3. (a) and (b) Examples of growth recipes where gas-phase reaction is decoupled from CNT growth. The preheater temperature in (a) is 600 °C and in (b) is 825 °C. (c) Height of CNT forests grown from the above recipes with various temperatures of preheater.

Thanks to the use of preheater, it was possible to grow CNT forests at a broad range of temperatures: from 550 to 825 °C (Figure 4a). Without preheater use, the growth at low

temperature is usually limited due to insufficient gas-phase decomposition. We expect the decoupling of gas-phase decomposition will be beneficial for the growth of high-density CNT forests at low temperature by minimizing the Ostwald ripening of the catalyst nanoparticles. Figure 4b is a scanning electron microscopy (SEM) image of a CNT forest grown with a decoupled gas phase recipe showing good alignment and high density.

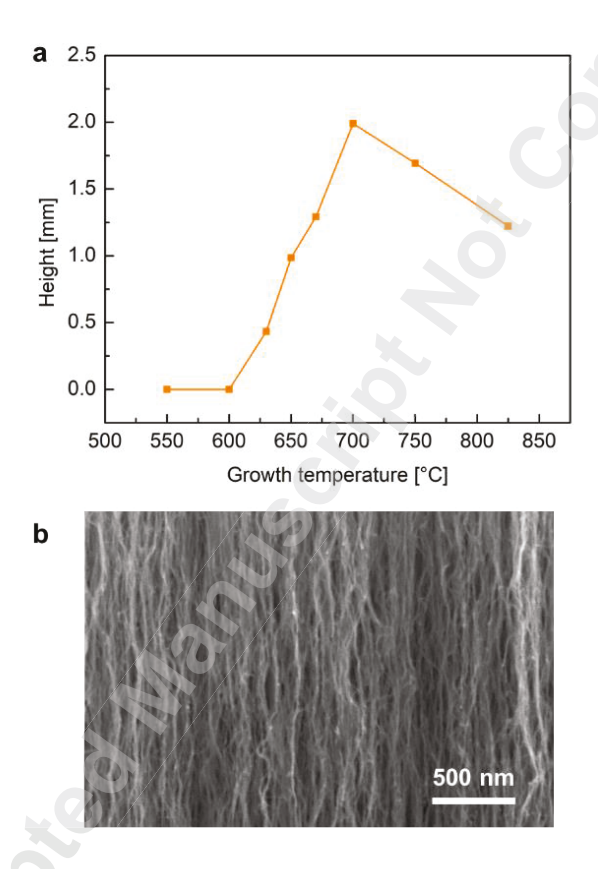


Figure 4. (a) Height of CNT forests grown at various growth temperature. In all the growths, the temperature of preheater was kept 825 °C. (b) A typical SEM image of a CNT forest.

7. Decoupling of catalyst formation

In this section, we present the effort to decouple catalyst formation step from catalytic CNT growth. By doing this, all the three steps (gas-phase decomposition, catalyst formation, and catalytic growth of CNTs) are now completely decoupled. Henceforth, the recipe where all these three steps are decoupled is referred to as "decoupled recipe". A typical example of the decoupled recipe is shown in Figure 5a. It includes a separate catalyst formation step prior to growth step. After formation of catalysts, the temperature of the growth zone is rapidly cooled down to around 200 °C. Then, the growth zone is rapidly ramped again to the target growth temperature. When the temperature reaches the target temperature, C₂H₄ is supplied to initiate the growth of CNTs. The approach to decouple catalyst formation in this way is enabled by the capability of the reactor to rapidly heat and cool the substrate.

To demonstrate whether the decoupled catalyst formation step does successfully form catalyst particles, we performed a control experiment. As a control experiment, we performed a growth with a recipe that does not have the decoupled catalyst formation step with all other conditions being identical (Figure 5b). The growth results clearly demonstrate the successful catalyst formation during the decoupled catalyst formation step. A millimeter-tall CNT forest was obtained from the decoupled recipe (Figure 5c), whereas no significant CNT forest was grown from the control recipe (Figure 5d).

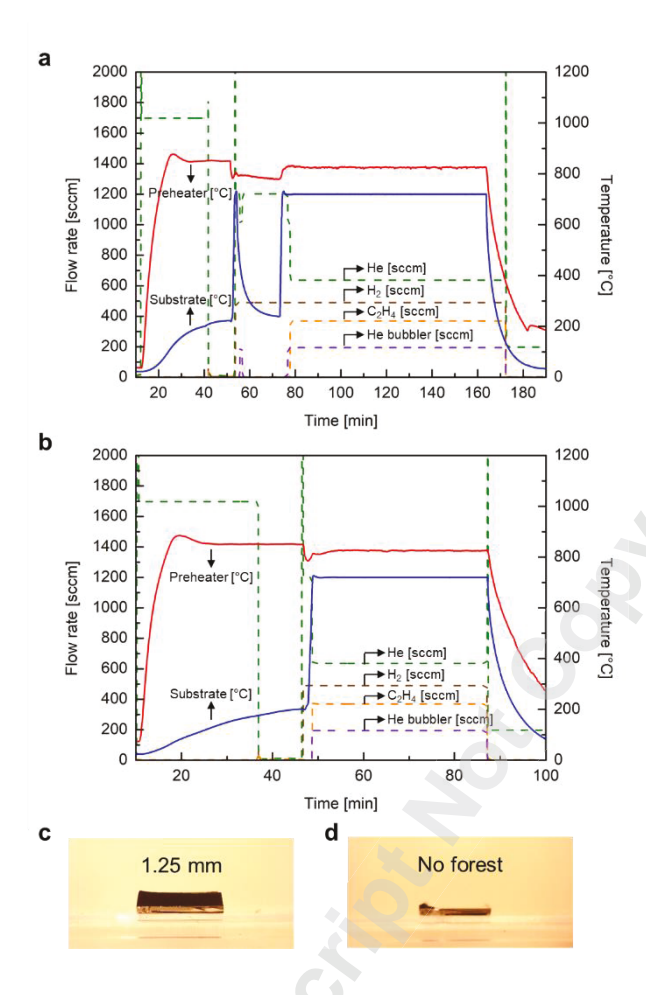


Figure 5. (a) Growth recipe with a decoupled catalyst formation step and (c) the image of the CNT forest grown using the recipe shown in (a). (b) Growth recipe without a catalyst formation step and (d) the image of CNT forest grown using the recipe shown in (b).

In a decoupled recipe, the number of parameters is much larger than conventional coupled recipes as the recipe consists of multiple steps. For example, it includes a cooling step after catalyst formation step and it has two ramping steps: one for catalyst formation and the other for CNT growth. Therefore, there is still room for optimizing these parameters. Here, we present initial parametric studies for the decoupled recipe. First, we tested the introduction timing of C₂H₄. In Figure 6a, C₂H₄ was supplied prior to the second ramping and in Figure 6b,

 C_2H_4 was supplied at the onset of growth step. In the latter recipe, which is usually used by most researchers, the concentration of decomposed hydrocarbon is 0 at the beginning of the growth stage and gradually increases to the target concentration. We anticipated that early introduction of C_2H_4 would be beneficial to the growth since it allows the growth step to begin at a desired concentration of decomposed hydrocarbon. Nevertheless, in this experiment, the early introduction of C_2H_4 did not result in a taller forest (Figure 6c and d). We believe that there is an optimum timing for the introduction of C_2H_4 , which will be further studied in the future.

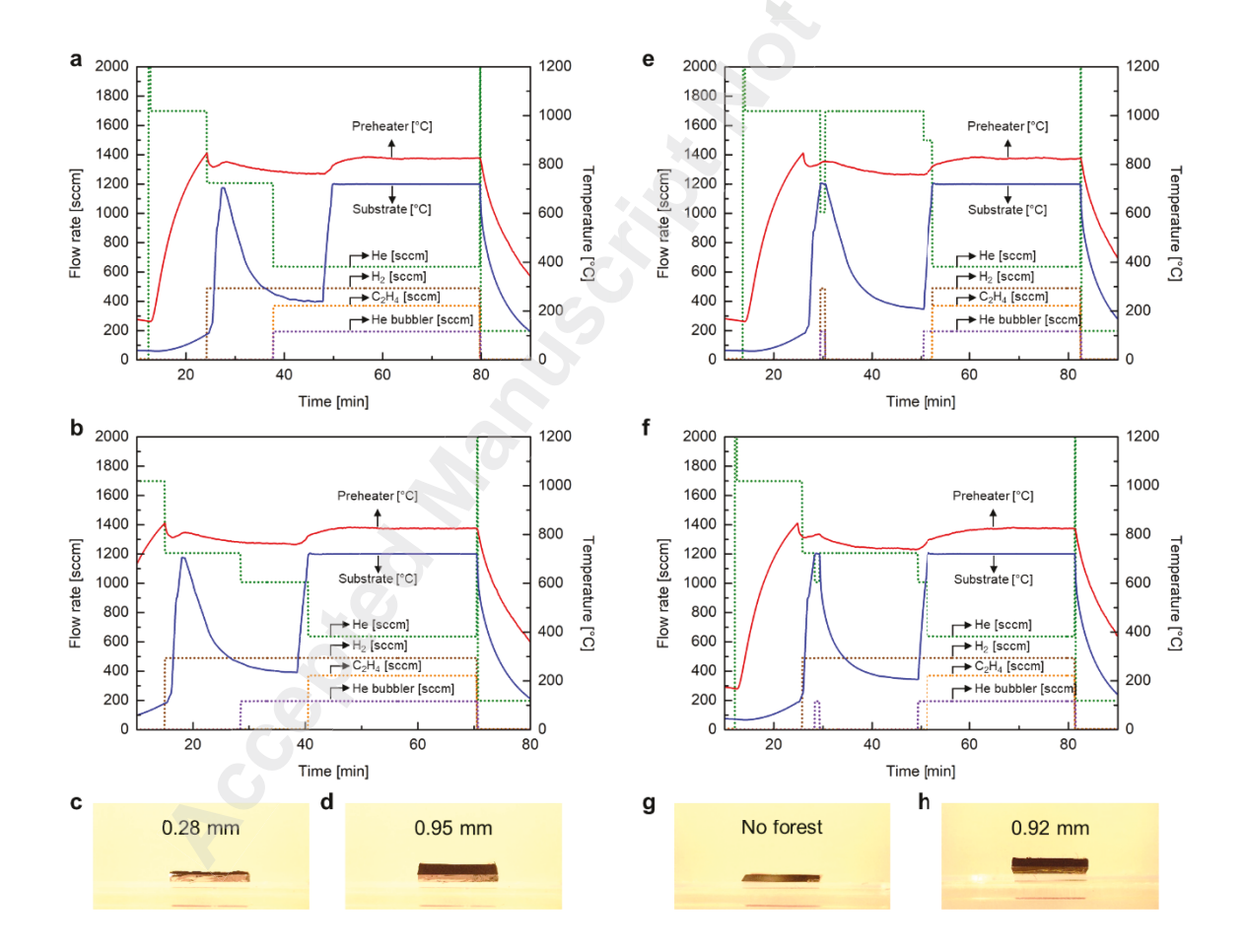


Figure 6. Decoupled recipes with different gas introduction timing. (a)-(d) Comparison of C₂H₄

introducing timing. (a) Dynamic recipe where C₂H₄ is supplied prior to the second ramping step and (c) the corresponding growth result. (b) Dynamic recipe where C₂H₄ is introduced at the beginning of growth step and (d) the corresponding growth result. (e)-(h) Comparison of H₂ introducing timing. (e) Dynamic recipe where the supply of H₂ is halted during the cooling step (g) the corresponding growth result. (f) Dynamic recipe where H₂ is continuously supplied

The supply of H₂ was also tested in our decoupled recipe. Since the decoupled recipes have a

during the cooling step and (h) the corresponding growth result.

"cooling" step between the catalyst formation and CNT growth, it was necessary to decide the gas composition during the cooling step. We compared two recipes which supplies only helium (Figure 6e) and hydrogen with helium (Figure 6f) during the cooling step. As a result, no CNT forest growth resulted when the hydrogen supply was halted during the cooling step, while a millimeter-tall uniform CNT forest was grown when hydrogen was supplied during the cooling step. Thus, once the catalyst particles are formed, exposing the substrate in a reducing atmosphere is desirable to keep the formed catalyst particles active, although further analysis of the catalyst particles are necessary to consolidate ideal gas supply in the decoupled recipes. The decoupled recipe was enabled by leveraging the ability to rapidly heat and cool the reactor. We tested the ramping rate in the first and the second ramping of the decoupled recipe. Figure 7 summarizes three combinations of first and second ramping rates. First, we programmed the recipe to ramp in 120 s in both the ramping steps. The temperature curves in Figure 7b and c show the successful ramping in 120 s, and growth of CNT forests was successful with this

17

combination of ramping rates (Figure 7d). When the first ramping rate was doubled (Figure 7e)

with the same second ramping rate (Figure 7f), the growth was still successful (Figure 7g).

Finally, when both the ramping steps were programmed to be in 60 s, the reactor was successfully heated in 60 s (Figure 7h and i), and the growth of CNT forest was still successful (Figure 7j). The results demonstrate the ability of our reactor to rapidly heat the substrate at a ramping rate as high as 12 °C/s. This ramping rate is much higher than those achievable from conventional resistive heater (typically less than 1 °C/s).

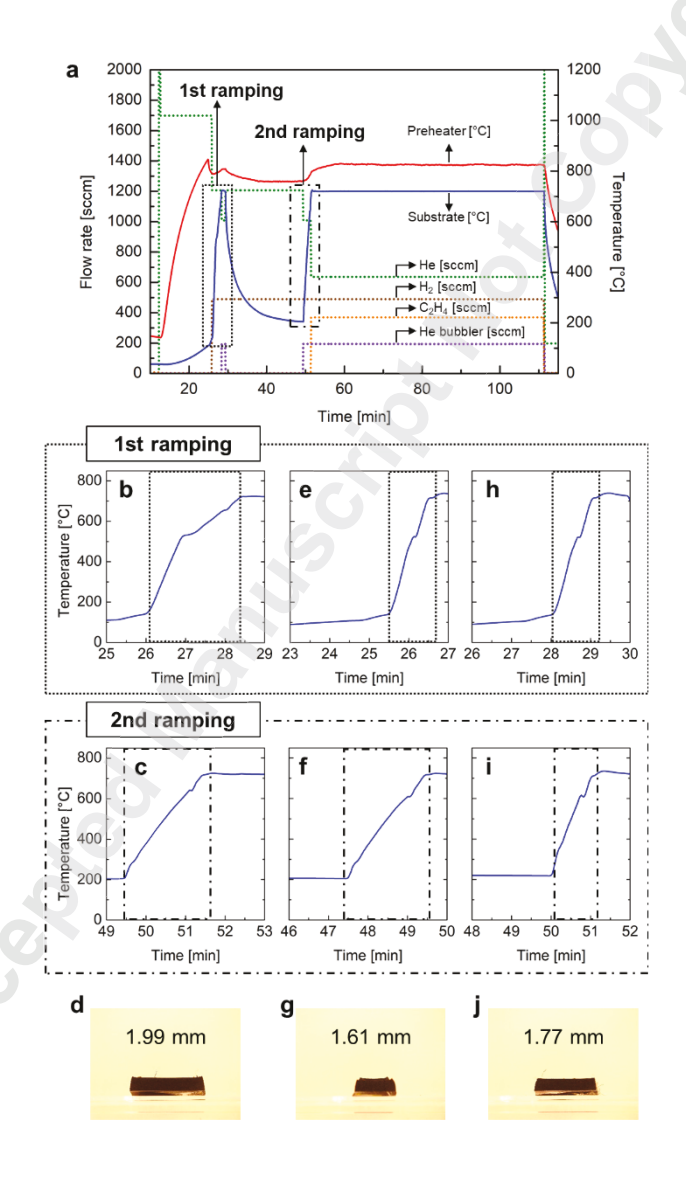


Figure 7. Decoupled recipes with three different combinations of first and second ramping rates.

(a) Overall shape of a reference decoupled recipe. (b)-(d) A growth with (b) first ramping in

18

Copyright © 2019 by ASME

120 s and (c) second ramping in 120 s and (d) the growth result. (e)-(g) A growth with (e) first

ramping in 60 s and (f) second ramping in 120 s and (g) the growth result. (h)-(j) A growth with

(h) first ramping in 60 s and (i) second ramping in 60 s and (j) the growth result.

There are two main benefits of the high controllability of rate of temperature change. First, at

high ramping rate as shown in Figure 7, we can study the pure effect of annealing temperature

and/or growth temperature, excluding the side effects during the ramping. Typically, with low

ramping rate, there occurs unwanted effects such as Ostwald ripening during a ramping step.

By minimizing the ramping time, we can mitigate these unintended effects during a ramping

step. Second, we can investigate the effect of ramping rate with the fixed annealing temperature

and/or growth temperature.

8. Improving growth consistency

As mentioned earlier, the main origin of inconsistent growth of CNT forest is oxygen-

containing molecules. Here, we take multiple measures to mitigate the effect of oxygen-

containing molecules. We perform air baking to clean the wall of reactor between growth runs.

The growth recipes always start with pumping down the reactor below 30 mTorr followed by

helium purging (denoted as "1st pumping" in Figure 8a).

19

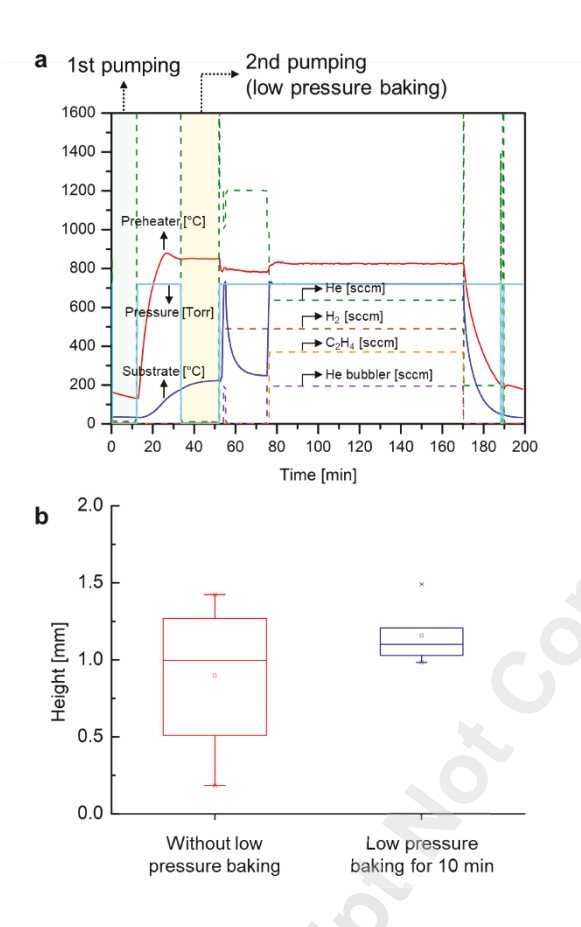


Figure 8. (a) Recipe of CNT forest growth that includes low pressure baking and (b) box plot of height of CNT forests grown from the recipe without low pressure baking and from the recipe with low pressure baking for 10 min.

In addition to these basic efforts, we added a second pumping, or low-pressure baking (denoted as "2nd pumping" in Figure 8a), before the catalyst formation step. After the first ramping, the preheater is heated to 850 °C. When the temperature is reached, affected by the heating of preheater, the temperature of growth zone increases to around 200 °C. At this moment, the reactor is pumped down again (for 10 min in Figure 8a while the time may be varied). The effect of this second pumping is shown in Figure 8b. Compared to the growth without the second pumping, the growth with second pumping resulted in taller CNT forests. Moreover,

the growths were more consistent; the coefficient of variation (defined as mean divided by

standard deviation) decreased from 0.49 to 0.13.

There is also room for further improvement in the consistency. For example, the period of the

low-pressure baking should be optimized. Since the catalyst formation step is decoupled in our

decoupled recipe, we can also study the effect of gas composition during catalyst formation

step on the growth consistency.

9. In situ measurement of growth kinetics

In situ optical imaging of forest growth is an easy and established method for directly obtaining

the growth kinetics [42,43]. Here we use a high definition video camera with a high enough

resolution to record and monitor the growth. The video camera is positioned to record the image

observed through a port in the reactor that is designed to be along the quartz tube axis. After

the growth has terminated, we use an image processing script to extract the forest height with

time as illustrated in Figure 9a. The forest height is then plotted with time to obtain the growth

curve (Figure 9b).

21

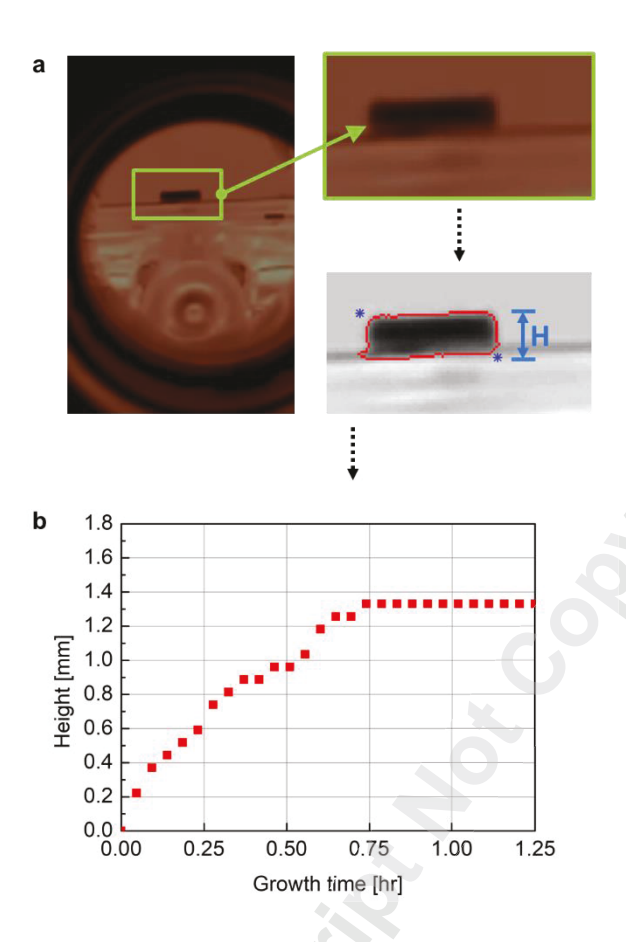


Figure 9. Image processing from the video of the growth of CNT forest and (b) the obtained growth curve.

10. Conclusions

In this work, we present our approaches aimed at solving the key challenges plaguing the manufacturing of carbon nanotube forests by leveraging the unique capabilities of our customized RTP-CVD reactor. We demonstrated the potential of decoupled recipes to independently control gas-phase decomposition, catalyst formation, and catalytic growth of CNTs. By using a separate resistive preheater, the gas-phase decomposition was decoupled from CNT growth. The decoupling of catalyst formation step was also demonstrated, which

was enabled by rapid thermal processing. The growth consistency was significantly improved by the efforts to reset the state of the reactor before every growth run by air baking between growth runs, pumping down, and additional low-pressure baking. Finally, we also presented the platform to study in situ kinetics of CNT forest growth by videography. We believe that the combined approach will solve the imminent challenges of control in height, density, and quality of CNT forest, and eventually contribute to the development of robust manufacturing processes for CNT forests.

Acknowledgments

This research was supported by the National Science Foundation (Award Number:1825772) and the Department of Industrial Engineering at the University of Pittsburgh. M. Bedewy is grateful for the Ralph E. Powe Junior Faculty Enhancement Award from Oak Ridge Associated Universities (ORAU). Characterization was performed, in part, at the Nanoscale Fabrication and Characterization Facility, a laboratory of the Gertrude E. and John M. Petersen Institute of NanoScience and Engineering, housed at the University of Pittsburgh.

References

- [1] Ebbesen, T. W., Lezec, H. J., Hiura, H., Bennett, J. W., Ghaemi, H. ., and Thio, T., 1996, "Electrical Conductivity of Individual Carbon Nanotubes," Nature, **382**, pp. 54–56.
- [2] Berber, S., Kwon, Y.-K., and Tomanek, D., 2000, "Unusually High Thermal Conductivity of Carbon Nanotubes," Phys. Rev. Lett., **84**(20), pp. 4613–4616.

23

- [3] Yu, M., Yu, M., Lourie, O., Dyer, M. J., Moloni, K., Kelly, T. F., and Ruoff, R. S., 2000, "Strength and Breaking Mechanism of Multiwalled Carbon Nanotubes Under Tensile Load," Science, **287**(2000), pp. 637–640.
- [4] Soga, I., Kondo, D., Yamaguchi, Y., Iwai, T., Kikkawa, T., and Joshin, K., 2009, "Thermal Management for Flip-Chip High Power Amplifiers Utilizing Carbon Nanotube Bumps," 2009 IEEE Int. Symp. Radio-Frequency Integr. Technol. RFIT 2009, pp. 221–224.
- [5] Vanpaemel, J., Sugiura, M., Barbarin, Y., De Gendt, S., Tökei, Z., Vereecken, P. M., and van der Veen, M. H., 2014, "Growth and Integration Challenges for Carbon Nanotube Interconnects," Microelectron. Eng., **120**, pp. 188–193.
- [6] Holt, J. K., Park, H. G., Wang, Y., Stadermann, M., Artyukhin, A. B., Grigoropoulos,
 C. P., Noy, A., and Bakajin, O., 2006, "Fast Mass Transport Through Sub-2 Nanometer Carbon Nanotubes," Science, 312(5776), pp. 1034–1037.
- [7] Liang, X., Shin, J., Magagnosc, D., Jiang, Y., Jin Park, S., John Hart, A., Turner, K., Gianola, D. S., and Purohit, P. K., 2017, "Compression and Recovery of Carbon Nanotube Forests Described as a Phase Transition," Int. J. Solids Struct., **122–123**, pp. 196–209.
- [8] Fan, S., Chapline, M. G., Franklin, N. R., Tombler, T. W., Cassell, A. M., and Dai, H., 1999, "Self-Oriented Regular Arrays of Carbon Nanotubes and Their Field Emission Properties," Science, **283**(5401), pp. 512–514.
- [9] Cho, W., Schulz, M., and Shanov, V., 2014, "Growth and Characterization of Vertically Aligned Centimeter Long CNT Arrays," Carbon, **72**, pp. 264–273.

- [10] Hata, K., Futaba, D. N., Mizuno, K., Namai, T., Yumura, M., and Iijima, S., 2004, "Water-Assisted Highly Efficient Synthesis of Impurity-Free Single-Walled Carbon Nanotubes," Science, 306(5700), pp. 1362–1364.
- [11] Seung Min Kim, Cary, L. P., Placidus, B. A., Dmitri, N. Z., Robert, H. H., Maruyama,
 B., and Stach, E. A., 2010, "Evolution in Catalyst Morphology Leads to Carbon
 Nanotube Growth Termination," J. Phys. Chem. Lett., 1(6), pp. 918–922.
- [12] Stadermann, M., Sherlock, S. P., In, J. B., Fornasiero, F., Park, H. G., Artyukhin, A. B., Wang, Y., De Yoreo, J. J., Grigoropoulos, C. P., Bakajin, O., Chernov, A. A., and Noy, A., 2009, "Mechanism and Kinetics of Growth Termination in Controlled Chemical Vapor Deposition Growth of Multiwall Carbon Nanotube Arrays," Nano Lett, 9(2), pp. 738–744.
- [13] Polsen, E. S., McNerny, D. Q., Viswanath, B., Pattinson, S. W., and John Hart, A., 2015, "High-Speed Roll-to-Roll Manufacturing of Graphene Using a Concentric Tube CVD Reactor," Sci. Rep., 5(1), p. 10257.
- [14] Guzmán De Villoria, R., Hart, A. J., and Wardle, B. L., 2011, "Continuous High-Yield Production of Vertically Aligned Carbon Nanotubes on 2D and 3D Substrates," ACS Nano, 5(6), pp. 4850–4857.
- [15] Lin, Z., Gui, X., Zeng, Z., Liang, B., Chen, W., Liu, M., Zhu, Y., Cao, A., and Tang, Z., 2015, "Biomimetic Carbon Nanotube Films with Gradient Structure and Locally Tunable Mechanical Property," Adv. Funct. Mater., **25**(46), pp. 7173–7179.
- [16] Lee, C. J., Son, K. H., Park, J., Yoo, J. E., Huh, Y., and Lee, J. Y., 2001, "Low Temperature Growth of Vertically Aligned Carbon Nanotubes by Thermal Chemical

- Vapor Deposition," Chem. Phys. Lett., **338**(2–3), pp. 113–117.
- [17] Jeong, H. J., Jeong, S. Y., Shin, Y. M., Han, J. H., Lim, S. C., Eum, S. J., Yang, C. W., Kim, N. G., Park, C. Y., and Lee, Y. H., 2002, "Dual-Catalyst Growth of Vertically Aligned Carbon Nanotubes at Low Temperature in Thermal Chemical Vapor Deposition," Chem. Phys. Lett., 361(3–4), pp. 189–195.
- [18] Meshot, E. R., Plata, L., Tawfick, S., Zhang, Y., Verploegen, E. a, and Hart, a J., 2009, "Engineering Vertically Aligned Carbon Nanotube Growth by Decoupled Thermal Treatment of Precursor and Catalyst," ACS Nano, 3(9), pp. 2477–2486.
- [19] Nessim, G. D., Seita, M., O'Brien, K. P., Hart, A. J., Bonaparte, R. K., Mitchell, R. R., and Thompson, C. V., 2009, "Low Temperature Synthesis of Vertically Aligned Carbon Nanotubes with Electrical Contact to Metallic Substrates Enabled by Thermal Decomposition of the Carbon Feedstock," Nano Lett., 9(10), pp. 3398–3405.
- [20] Youn, S. K., Frouzakis, C. E., Gopi, B. P., Robertson, J., Teo, K. B. K., and Park, H. G., 2013, "Temperature Gradient Chemical Vapor Deposition of Vertically Aligned Carbon Nanotubes," Carbon, 54, pp. 343–352.
- [21] Yang, N., Youn, S. K., Frouzakis, C. E., and Park, H. G., 2018, "An Effect of Gas-Phase Reactions on the Vertically Aligned CNT Growth by Temperature Gradient Chemical Vapor Deposition," Carbon, **130**, pp. 607–613.
- [22] Sakurai, S., Inaguma, M., Futaba, D. N., Yumura, M., and Hata, K., 2013, "Diameter and Density Control of Single-Walled Carbon Nanotube Forests by Modulating Ostwald Ripening through Decoupling the Catalyst Formation and Growth Processes," Small, 9(21), pp. 3584–3592.

- [23] Sakurai, S., Inaguma, M., Futaba, D. N., Yumura, M., and Hata, K., 2013, "A Fundamental Limitation of Small Diameter Single-Walled Carbon Nanotube Synthesis-a Scaling Rule of the Carbon Nanotube Yield with Catalyst Volume," Materials (Basel)., 6(7), pp. 2633–2641.
- [24] Li, J., Bedewy, M., White, A. O., Polsen, E. S., Tawfick, S., and John Hart, A., 2016, "Highly Consistent Atmospheric Pressure Synthesis of Carbon Nanotube Forests by Mitigation of Moisture Transients," J. Phys. Chem. C, **120**(20), p. 11277–11287.
- [25] Oliver, C. R., Polsen, E. S., Meshot, E. R., Tawfick, S., Park, S. J., Bedewy, M., and Hart, A. J., 2013, "Statistical Analysis of Variation in Laboratory Growth of Carbon Nanotube Forests and Recommendations for Improved Consistency," ACS Nano, 7(4), pp. 3565–3580.
- [26] In, J. Bin, Grigoropoulos, C. P., Chernov, A. A., and Noy, A., 2011, "Hidden Role of Trace Gas Impurities in Chemical Vapor Deposition Growth of Vertically-Aligned Carbon Nanotube Arrays," Appl. Phys. Lett., 98(15), p. 153102.
- [27] In, J. Bin, Grigoropoulos, C. P., Chernov, A. A., and Noy, A., 2011, "Growth Kinetics of Vertically Aligned Carbon Nanotube Arrays in Clean Oxygen-Free Conditions," ACS Nano, 5(12), pp. 9602–9610.
- [28] Shi, W., Li, J., Polsen, E. S., Oliver, C. R., Zhao, Y., Meshot, E. R., Barclay, M., Fairbrother, D. H., Hart, A. J., and Plata, D. L., 2017, "Oxygen-Promoted Catalyst Sintering Influences Number Density, Alignment, and Wall Number of Vertically Aligned Carbon Nanotubes," Nanoscale, 9, pp. 5222–5233.
- [29] Bedewy, M., Meshot, E. R., Reinker, M. J., and Hart, A. J., 2011, "Population Growth

- Dynamics of Carbon Nanotubes," ACS Nano, 5(11), pp. 8974–8989.
- [30] Bedewy, M., and Hart, A. J., 2013, "Mechanical Coupling Limits the Density and Quality of Self-Organized Carbon Nanotube Growth," Nanoscale, 5(7), p. 2928.
- [31] Balakrishnan, V., Bedewy, M., Meshot, E. R., Pattinson, S. W., Polsen, E. S., Laye, F., Zakharov, D. N., Stach, E. A., and Hart, A. J., 2016, "Real-Time Imaging of Self-Organization and Mechanical Competition in Carbon Nanotube Forest Growth," ACS Nano, **10**(12), pp. 11496–11504.
- [32] Bedewy, M., Farmer, B., and Hart, A. J., 2014, "Synergetic Chemical Coupling Controls the Uniformity of Carbon Nanotube Microstructure Growth," ACS Nano, **8**(6), pp. 5799–5812.
- [33] Bedewy, M., Meshot, E. R., Guo, H., Verploegen, E. A., Lu, W., and Hart, A. J., 2009, "Collective Mechanism for the Evolution and Self-Termination of Vertically Aligned Carbon Nanotube Growth," J. Phys. Chem. C, **113**(48), pp. 20576–20582.
- [34] Bedewy, M., Meshot, E. R., and Hart, A. J., 2012, "Diameter-Dependent Kinetics of Activation and Deactivation in Carbon Nanotube Population Growth," Carbon, **50**(14), pp. 5106–5116.
- [35] Zhong, G., Iwasaki, T., Robertson, J., and Kawarada, H., 2007, "Growth Kinetics of 0.5 Cm Vertically Aligned Single-Walled Carbon Nanotubes," J. Phys. Chem. B, 111(8), pp. 1907–1910.
- [36] Li, X., Zhang, X., Ci, L., Shah, R., Wolfe, C., Kar, S., Talapatra, S., and Ajayan, P. M., 2008, "Air-Assisted Growth of Ultra-Long Carbon Nanotube Bundles," Nanotechnology, 19(45), p. 455609.

- [37] Yasuda, S., Futaba, D. D. N., Yamada, T., Satou, J., Shibuya, A., Takai, H., Arakawa, K., Yumura, M., and Hata, K., 2009, "Improved and Large Area Single-Walled Carbon Nanotube Forest Growth by Controlling the Gas Flow Direction," ACS Nano, 3(12), pp. 4164–4170.
- [38] Zhang, Y., Gregoire, J. M., Dover, R. B. Van, and Hart, A. J., 2010, "Ethanol-Promoted High-Yield Growth of Few-Walled Carbon Nanotubes," J. Phys. Chem. C, 114(14), pp. 6389–6395.
- [39] Kim, H., Kang, J., Kim, Y., Hong, B. H., Choi, J., and Iijima, S., 2011, "Synthesis of Ultra-Long Super-Aligned Double-Walled Carbon Nanotube Forests," J. Nanosci. Nanotechnol., **11**(1), pp. 470–473.
- [40] Lee, J., Oh, E., Kim, T., Sa, J. H., Lee, S. H., Park, J., Moon, D., Kang, I. S., Kim, M. J., Kim, S. M., and Lee, K. H., 2015, "The Influence of Boundary Layer on the Growth Kinetics of Carbon Nanotube Forests," Carbon, 93, pp. 217–225.
- [41] Qi, J. L., Wang, X., Zheng, W. T., Liu, J. W., Tian, H. W., Li, Z. P., and Liu, C., 2008, "Influence of Oxygen on the Growth of Carbon Nanotubes," J. Phys. D Appl. Phys, 41, pp. 205306–6.
- [42] Puretzky, A. A., Eres, G., Rouleau, C. M., Ivanov, I. N., and Geohegan, D. B., 2008, "Real-Time Imaging of Vertically Aligned Carbon Nanotube Array Growth Kinetics," Nanotechnology, **19**(5), p. 055605.
- [43] Hart, A. J., Van Laake, L., and Slocum, A. H., 2007, "Desktop Growth of Carbon-Nanotube Monoliths with in Situ Optical Imaging," Small, 3(5), pp. 772–777.

List of Figure Captions

Figure 1. Height of representative CNT forests. References: Fan 1999 [8], Hata 2004 [10], Zhong 2007 [35], Ajayan 2008 [36], Hata 2009 [37], Hart 2010 [38], Choi 2011 [39], Shanov 2014 [9], and Lee 2015 [40].

Figure 2. Schematic representation of our custom-designed rapid thermal processing CVD reactor.

Figure 3. (a) and (b) Examples of growth recipes where gas-phase reaction is decoupled from CNT growth. The preheater temperature in (a) is 600 °C and in (b) is 825 °C. (c) Height of CNT forests grown from the above recipes with various temperatures of preheater.

Figure 4. (a) Height of CNT forests grown at various growth temperature. In all the growths, the temperature of preheater was kept 825 °C. (b) A typical SEM image of a CNT forest.

Figure 5. (a) Growth recipe with a decoupled catalyst formation step and (c) the image of the CNT forest grown using the recipe shown in (a). (b) Growth recipe without a catalyst formation step and (d) the image of CNT forest grown using the recipe shown in (b).

Figure 6. Decoupled recipes with different gas introduction timing. (a)-(d) Comparison of C₂H₄ introducing timing. (a) Dynamic recipe where C₂H₄ is supplied prior to the second ramping step and (c) the corresponding growth result. (b) Dynamic recipe where C₂H₄ is introduced at the beginning of growth step and (d) the corresponding growth result. (e)-(h) Comparison of H₂ introducing timing. (e) Dynamic recipe where the supply of H₂ is halted during the cooling step (g) the corresponding growth result. (f) Dynamic recipe where H₂ is continuously supplied during the cooling step and (h) the corresponding growth result.

Figure 7. Decoupled recipes with three different combinations of first and second ramping rates.

30

(a) Overall shape of a reference decoupled recipe. (b)-(d) A growth with (b) first ramping in 120 s and (c) second ramping in 120 s and (d) the growth result. (e)-(g) A growth with (e) first ramping in 60 s and (f) second ramping in 120 s and (g) the growth result. (h)-(j) A growth with

(h) first ramping in 60 s and (i) second ramping in 60 s and (j) the growth result.

Figure 8. (a) Recipe of CNT forest growth that includes low pressure baking and (b) box plot of height of CNT forests grown from the recipe without low pressure baking and from the recipe with low pressure baking for 10 min.

Figure 9. Image processing from the video of the growth of CNT forest and (b) the obtained growth curve.